SIMULATION OF TEMPERATURE AND STRESS FIELDS DURING RCC DAM CONSTRUCTION

By Ronaldo Luna[1] and Yong Wu[2]

ABSTRACT: The worldwide experience in the construction of roller-compacted concrete (RCC) dams together with the use of numerical solutions, allows the simulation of different scenarios in a computer. It is well documented that thermal control is one of the most important problems for RCC dam construction. The dam temperature changes due to the heat produced by the internal hydration of concrete and the environmental boundary conditions influencing the elastic modulus and creep properties of concrete. The construction process was simulated to study how the temperature and stress change during dam construction. The numerical methodology considers the effect of temperature on the elastic modulus and the creep behavior of concrete. A 3D finite-element program was developed to simulate the construction process. An engineering application of this methodology is presented by simulating the construction of an RCC gravity dam in southern China. The results show how the temperature and stress change with the construction process. The results also show that it is feasible to build RCC dams in low temperature seasons without additional temperature control measures.

INTRODUCTION

Roller-compacted concrete (RCC) dams consist of concrete placed at a lower water-to-cement ratio as compared to conventional concrete with the aid of compaction equipment and methodologies normally employed for earth fill placement. It involves basically building a concrete gravity dam by methods usually associated with earth dam construction (Hansen 1996). This construction method permits a considerable reduction of costs and construction time of dams, compared not only with traditional concrete dams, but also with earth fill dams. The American Concrete Institute (ACI) defines RCC as ''concrete compacted by roller compaction that, in its unhardened state, will support a roller while being compacted.'' The factors that affect the material properties of RCC are the same as those that affect the properties of conventional concrete, which are water-to-cement ratio, quality of mixing ingredients, and degree of consolidation and curing. The main difference between RCC and conventional concrete is the mixture consistency and the method of consolidation [U.S. Army Corps of Engineers (U.S. ACE) 1993]. In comparing RCC with conventional concrete, less water and consequently less cement is required to produce an equivalent water-to-cement ratio (Hansen 1996). Because less cement is used, the hydration heat produced by RCC is much less than that produced by conventional concrete. Therefore, the rate of hydration process is slower in RCC (Schrader 1988). This aids in reducing the peak temperature and thermal induced cracking. RCC dams are built in thin lifts, and the construction process of RCC dams is much easier than that of conventional concrete dams.

RCC has gained worldwide acceptance as an alternative to conventional concrete in dam construction due to the construction advantages and proved performance. One of the early uses of RCC was in 1974 for the rehabilitation of the Tarbela Dam in Pakistan where the material was named ''rollcrete.'' RCC gained acceptance internationally in the United States after extensive laboratory and field tests by the U.S. ACE and the U.S. Bureau of Reclamation. In 1982, the Willow Creek Dam in Oregon was completed to a total dam height of 52 m (Hansen 1996). Low costs and rapid construction make RCC dams more advantageous than any other type of dam construction (U.S. ACE 1992). By the end of 1997, a total of 150 projects were completed using RCC construction (Hansen 1997). There is now sufficient confidence in the RCC dam method of construction not only for gravity dams but also for arch-gravity dams (Dunstan 1999).

In the design and construction of RCC dams, the thermal stresses and temperature control measures have to be seriously considered. In the lessons learned from the Upper Stillwater Dam in Utah, the thermal-induced cracks originated at the crest and propagated into the RCC mass. The cracks did not produce a stability or seepage problem because they were repaired using polyurethane resin in two contracts (Smoack 1991). After construction, performance plays an important role on the stresses of structures. However, the temperature during the construction period should also be studied because this is where the hydration temperature effects are most active. These temperature differentials induce cracks in the structures, which harm their integrity, permeability, and durability.

Generally, there are no cooling pipes embedded in RCC dams, and heat can only dissipate through the top surface of the concrete. Therefore, the inner core of the dam is almost adiabatic and the temperature rise is significant. These changes in temperature will induce considerable thermal stresses to be considered in the design of the massive concrete structures.

Temperature has a significant effect on creep. First, the ultimate elastic modulus of concrete is not significantly affected by temperature (Zhu et al. 1976), but the temperature rise accelerates the initial elastic modulus of concrete. Second, the creep rate also increases with increased temperature, and consequently the creep strain also increases (Bazant 1982). Therefore, the elastic modulus and creep at different points in the RCC dam are all functions of temperature.

Because RCC dams are constructed in lifts, the gravity stresses accumulate with each lift. On the other hand, the thermal stresses will also accumulate with time as the increase of concrete volume occurs. Furthermore, the properties of concrete are a function of time. Different lifts with different ages have different mechanical, thermal, and creep properties. Therefore, to study how the temperature and stress change, it is necessary to simulate the construction process of RCC dams in both the spatial (3D) and temporal domain.

[1]Assoc. Prof., Dept. of Civ. Engrg., Univ. of Missouri at Rolla, 1870 Miner Circle, Rolla, MO 65409.

[2]Grad. Student, Dept. of Civ. Engrg., Univ. of Missouri at Rolla, 1870 Miner Circle, Rolla, MO.

Note. Discussion open until March 1, 2001. To extend the closing date one month, a written request must be filed with the ASCE Manager of Journals. The manuscript for this paper was submitted for review and possible publication on August 20, 1999. This paper is part of the ***Journal of Construction Engineering and Management***, Vol. 126, No. 5, September/October, 2000. ©ASCE, ISSN 0733-9634/00/0005-0381–0388/ $8.00 + $.50 per page. Paper No. 21722.

UNSTEADY THERMAL AND CREEP STRESSES

Unsteady Temperature

The sources of heat generated during the construction of an RCC dam are due to hydration of concrete and the boundary environmental conditions, both of which change with time. The temperature also changes with time developing an unsteady-state problem within the mass concrete. A concrete structure with heat generating internally can be subjected to various types of boundary conditions: (1) Specified temperature; (2) specified flux; and (3) convective-type, as shown in Fig. 1, as C_1, C_2, and C_3, respectively. The specified temperature condition C_1 refers to the instance when that boundary temperature is given. The specified flux condition C_2 refers to the type of temperature flow through the boundary, and the adiabatic condition is often used in mass concrete structures, referring to no heat flow across the boundary. When the concrete surfaces are exposed to air or water, then the convective-type condition C_3 is applied. This boundary condition describes heat transfer from the concrete surface to a moving fluid, and the rate of heat transfer is proportional to the temperature difference between the concrete surface and the moving fluid (Mills 1999).

The governing equation of the unsteady temperature problem can be derived from the energy conservation principle and Fourier law of heat conduction. The following equation and corresponding boundary conditions govern the temperature change in 3D space and time:

$$\frac{\partial}{\partial x}\left(a_x \frac{\partial T}{\partial x}\right) + \frac{\partial}{\partial y}\left(a_y \frac{\partial T}{\partial y}\right) + \frac{\partial}{\partial z}\left(a_z \frac{\partial T}{\partial z}\right) + \frac{\partial \theta}{\partial t} - \frac{\partial T}{\partial t} = 0 \quad (1)$$

where a_x, a_y, and a_z = material thermal diffusivity.

$$T = T_0(x, y, z), \quad \text{when } t = 0 \quad (2a,b)$$

On boundary C_1, the temperature is known, and this is a specified temperature condition

$$T = T_b(t) \quad \text{on boundary } C_1 \quad (3)$$

On boundary C_2, the adiabatic condition is satisfied, and it is the specified flux condition when the flux is equal to 0

$$\frac{\partial T}{\partial n} = 0 \quad \text{on boundary } C_2 \quad (4)$$

On boundary C_3, the convective-type condition is applied

$$\lambda_x \frac{\partial T}{\partial x} l_x + \lambda_y \frac{\partial T}{\partial y} l_y + \lambda_z \frac{\partial T}{\partial z} l_z = -\beta(T - T_c) \quad (5)$$

where T = transient temperature; θ = adiabatic temperature rise of concrete; t = time; T_0 = initial temperature; n = outer normal of the boundary; λ_x, λ_y, and λ_z = thermal conductivities; β = surface exothermic coefficient; T_c = temperature of the bounding fluid; l_x, l_y, and l_z = direction cosines of the external normal to the boundary.

The above problem can be solved in 3D using the finite-element method (FEM), and the equations for the FEM are listed as follows:

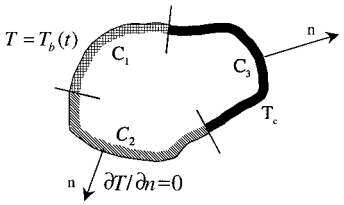

FIG. 1. Boundary Conditions on Solid Region

$$\left[H + \frac{2}{\Delta t} P\right]\{T\}_t + \left[H - \frac{2}{\Delta t} P\right]\{T\}_{t-\Delta t} + \{Q\}_{t-\Delta t} + \{Q\}_t = 0 \quad (6)$$

where

$$H_{ij} = \sum_e h_{ij}^e = \sum_e \iiint_{\Delta V} \left(a_x \frac{\partial N_i}{\partial x}\frac{\partial N_j}{\partial x} + a_y \frac{\partial N_i}{\partial y}\frac{\partial N_j}{\partial y} + a_z \frac{\partial N_i}{\partial z}\frac{\partial N_j}{\partial z}\right) \cdot dx\, dy\, dz$$

$$P_{ij} = \sum_e p_{ij}^e = \sum_e \iiint_{\Delta V} N_i N_j\, dx\, dy\, dz$$

$$Q_{ij} = \sum_e q_i^e = \sum_e \left(-\iiint_{\Delta V} \frac{\partial \theta}{\partial t} N_i\, dx\, dy\, dz - \iint_{\Delta S} \overline{\beta} T_c N_i\, ds + \left(\iint_{\Delta S} \overline{\beta} N_i [N_i N_j \cdots]\, ds\right) \begin{Bmatrix} T_i \\ T_j \\ \vdots \end{Bmatrix}\right)$$

Therefore, if the temperature at time $t - \Delta t$ is known, then the temperature at time t can be calculated, because if the initial temperature is known, the temperature at any time can be calculated.

Creep Stress with Temperature Effects

Creep is a very complex problem that has been studied extensively. The most widely used models for creep analysis are the Comité Euro-International du Béton-Fédération Internationale de la Precontrainte (CEB-FIP) model (CEB-FIP 1978), the ACI model (ACI 1978); the Bazant and Panula model (Bazant 1982), and the Exponential model (Bazant and Wu 1973). Due to its formulation, the Exponential model is the only one that can avoid storing the whole stress history resulting in an increased efficiency in the numerical implementation of this concrete phenomenon. The computer program developed for the simulation of construction was based on the following mathematical formulation. The Exponential model of creep compliance can be expressed with the Dirichlet series (Bazant and Wu 1973) as

$$J(t, \tau) = \sum_{k=1}^{N} \frac{1}{C_k(\tau)} [1 - \exp(y_k(\tau) - y_k(t))] \quad (7)$$

where $J(t, \tau)$ = creep function; and τ = loading age in days. For mass concrete structures, the following specific form is often used:

$$J(t, \tau) = \frac{1}{E(\tau)} + C(t, \tau) \quad (8a)$$

$$C(t, \tau) = \sum_{i=1}^{2} (A_i + B_i \tau^{-G_i})[1 - \exp(-S_i(t - \tau))] + D[\exp(-S_3\tau) - \exp(-S_3 t)] \quad (8b)$$

$$E(\tau) = E_0(1 - \exp(-\alpha\tau^{\beta})) \quad (8c)$$

where $C(t, \tau)$ = creep compliance; $E(\tau)$ and E_0 = transient and ultimate elastic moduli, respectively; A_i, B_i, G_i, S_i, D, α, and β = all experimental fitting parameters.

To consider the effects of temperature on elastic modulus and creep behavior of concrete, Du and Liu (1994) introduced the term equivalent age τ_e to replace the actual concrete age. After a long derivation, the final formulas of creep strain and stress in 3D are presented as follows [for details, refer to Du and Liu (1994)].

Let the time interval $[t_0, t]$ be subdivided into N steps, then

J. Constr. Eng. Manage., 2000, 126(5): 381-388

the creep strain increment $\{\Delta\varepsilon_n^C\}$ at a typical step $[t_{n-1}, t_n]$ ($n = 1, 2, \ldots, N$) can be expressed as

$$\{\Delta\varepsilon_n^C\} = [Q]\sum_{r=1}^{3}[(1 - \exp(-S_r\varphi_{Tn}\Delta\tau_n))\{\omega_{rn}\} + \{\Delta\sigma_n\}\varphi_{rn}^* h_{rn}^*]$$

$$= [\eta_n] + q_n[Q]\{\Delta\sigma_n\} \tag{9}$$

where

$$[Q] = \begin{bmatrix} 1 & -\mu & -\mu & 0 & 0 & 0 \\ & 1 & -\mu & 0 & 0 & 0 \\ & & 1 & 0 & 0 & 0 \\ & & & 2(1+\mu) & 0 & 0 \\ & & \text{Sym.} & & 2(1+\mu) & 0 \\ & & & & & 2(1+\mu) \end{bmatrix},$$

μ is the Poisson's ratio

$$\{\eta_n\} = \sum_{r=1}^{3}(1 - \exp(-S_r\varphi_{Tn}\Delta\tau_n))\{\omega_{rn}\}$$

$$q_n = \sum_{r=1}^{3}\varphi_{rn}^* h_{rn}^*$$

$$\{\omega_{rn}\} = \{\omega_{rn-1}\}\exp(S_r\varphi_{Tn-1}\Delta\tau_{n-1}) + [Q]\{\Delta\sigma_{n-1}\}\varphi_{rn-1}^* f_{rn-1}^* \cdot \exp(-S_r\Delta\tau_{n-1})$$

$$\varphi_{rn}^* = \varphi_r(\tau_{en-1/2})$$

$$h_{rn}^* = 1 - f_{rn}^* \exp\left(-S_r\sum_{i=1}^{n}\varphi_{Ti}\Delta\tau_i\right)$$

$$f_{rn}^* = \frac{1}{\Delta\tau_n}\int_{t_{n-1}}^{t_n}\exp\left(S_r\int_{t_0}^{\tau}\varphi_T\,dt'\right)d\tau$$

$$\Delta\tau_n = t_n - t_{n-1}$$

After the creep strain increment is calculated, the corresponding stress increment can be obtained

$$\{\Delta\sigma_n\} = [\overline{D_n}](\{\Delta\varepsilon_n\} - \{\eta_n\} - \{\Delta\varepsilon_n^T\}) \tag{10}$$

where $\{\Delta\varepsilon_n^T\}$ is the thermal strain; $[\overline{D_n}] = [D_n]/(1 + q_nE_n)$, in which $[D_n]$ = elastic matrix of the nth time interval, and E_n = elastic modulus.

The total stress at the moment of the nth step is

$$\{\sigma_n\} = \{\sigma_{n-1}\} + \{\Delta\sigma_n\} \tag{11}$$

Numerical Implementation

Based on the unsteady temperature and creep analysis shown above, a 3D FEM program was developed. The program can update the geometry of concrete structures dynamically during the computations simulating the construction process of an RCC layered dam. Temperature and stress distributions at different times form part of the analytical output. The writers have published a related article presenting the details of the numerical implementation of the methodology summarized in the previous section (Wu and Luna 2000).

CONSTRUCTION ENGINEERING APPLICATION

Project Description

Hydraulic dams are major structures that form part of the national infrastructure system that brings livelihood and energy to the civilian population. Many developing countries are building this type of infrastructure such as the Jinagya hydraulic project and the RCC dam located in the middle of the Loushui River, Zhili County, Hunan Province in China (Fig. 2). The dam's main function is to control floods; however, it also provides energy, irrigation, water supply, and navigation to nearby human settlements. This project is central for the development of the Loushui River, and the RCC gravity dam is the principal control structure. The maximum height of the

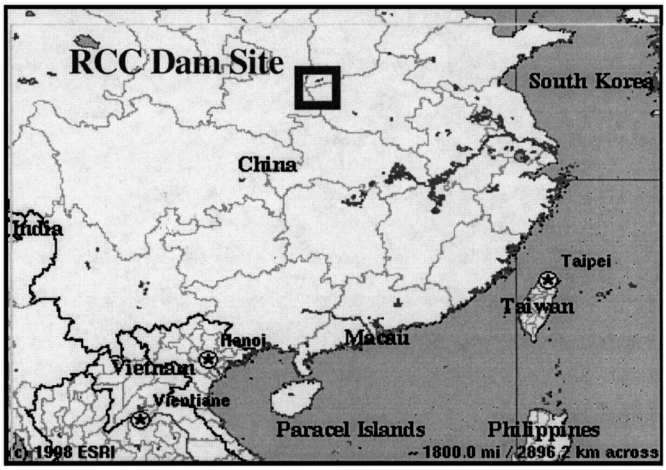

FIG. 2. Vicinity Map and RCC Dam Site Location

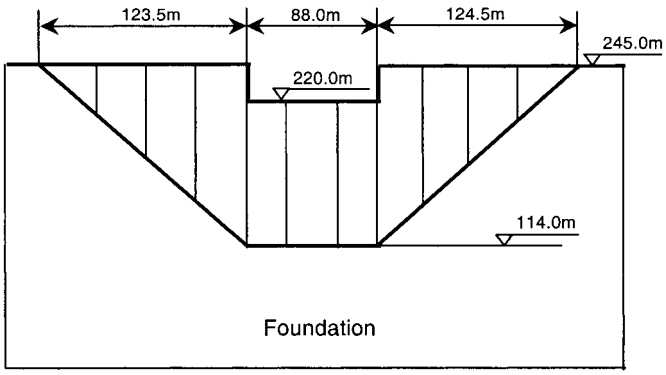

FIG. 3. Schematic Diagram of Dam from Upstream Point of View

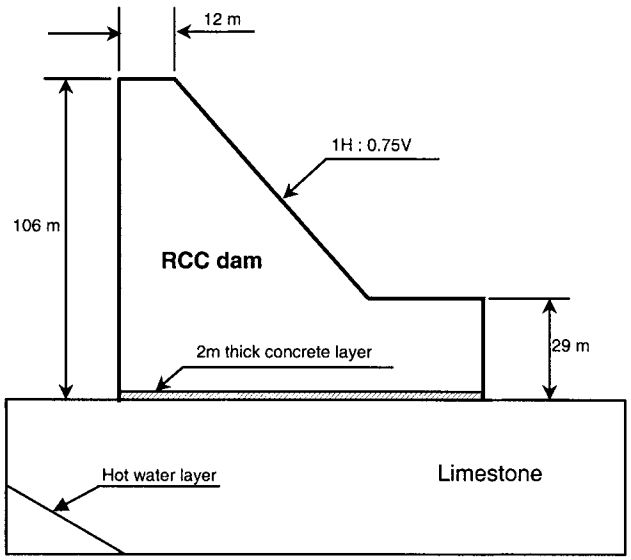

FIG. 4. Simplified Cross Section of Overflow Dam

J. Constr. Eng. Manage., 2000, 126(5): 381-388

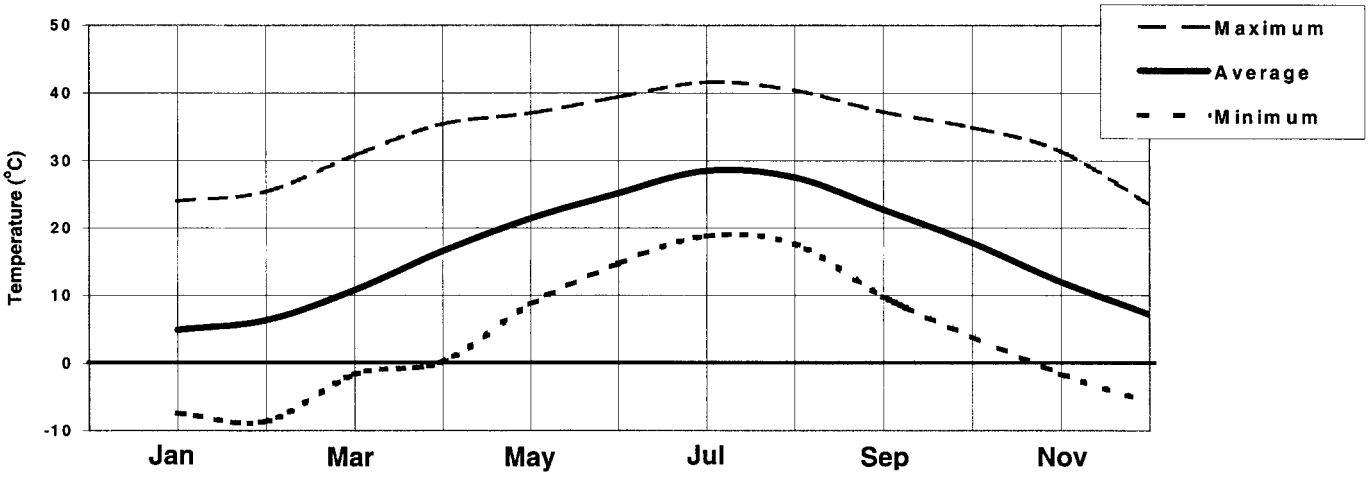

FIG. 5. Climatic Conditions at Dam Site

dam is 128 m, and the maximum width at the top is 12 m and at the bottom is 105 m. The maximum length of the dam is 336 m (Zhang 1995). The dam consists of non-overflow and overflow sections. The overflow section is in the middle of the dam, and it includes three segments. The maximum width of the segment is 33 m. The schematic diagram of the dam from the upstream point of view is shown in Fig. 3. To study how the temperature and stress fields affect the construction of the dam, the 3D FEM program was used to analyze this dam. Because the dam consists of segments or sections separated by vertical joints, the overflow segment with the maximum width was selected for the analysis. The construction process of the dam was simulated using the previously described computer program.

The foundation of the dam is in the Permian system limestone known as a formation with high compressive strength. There is a hot water layer in the foundation that remains constant at a temperature of 45°C. A 2-m-thick conventional concrete layer was placed between the RCC concrete and the foundation as a leveling surface. The simplified cross section of the overflow segment is shown in Fig. 4.

Climatic Conditions and Construction Schedule

The project site is located in south China at an approximate geographic longitude and latitude of 110.5° E and 29.5° N, respectively. The site elevation is at about 114 m above mean sea level. The peak high temperatures occur in July, and the low is in January. Typical weather conditions were provided by the Hunan Hydroelectric Investigation and Design Institute (Zhang 1995) and is plotted in Fig. 5 showing average, maximum, and minimum temperatures. The climatic conditions at the dam site are shown in Fig. 5, and the assumed construction schedule is known in Table 1.

As mentioned before, RCC dams are constructed in thin lifts. To simulate the construction process of the dam a thickness of lift was determined based on the anticipated RCC lifts at average conditions for a 10-day construction period. No artificial temperature control methods were anticipated, and the initial temperature of each lift is set to be equal to the climatic temperature at the time when it is constructed. Because the climatic temperatures at the dam site during the summer season (May to September) are relatively high, the construction will be stopped in these months to avoid the high initial temperature. The placement of RCC begins at the beginning of December, and the whole duration will be about 1.5 years provided that no major delays are incurred.

TABLE 1. RCC Dam Construction Schedule and Associated Initial Temperature

Layer number (1)	RCC placement schedule (2)	Elevation of top surface (m) (3)	Initial temperature (°C) (4)
1	Dec. 10	116.0	7.20
2	Jan. 1	119.0	4.92
3	Jan. 10	122.0	4.92
4	Jan. 20	125.0	4.92
5	Jan. 31	128.0	4.92
6	Feb. 10	131.0	6.34
7	Feb. 20	134.0	6.34
8	Feb. 28	137.0	6.34
9	Mar. 10	140.0	10.78
10	Mar. 20	143.0	10.78
11	Mar. 31	146.0	10.78
12	Apr. 10	149.0	16.57
13	Apr. 20	152.0	16.57
14	Oct. 1	155.0	17.76
15	Oct. 10	158.0	17.76
16	Oct. 20	161.0	17.76
17	Oct. 31	164.0	17.76
18	Nov. 10	167.0	11.96
19	Nov. 20	170.0	11.96
20	Nov. 30	173.0	11.96
21	Dec. 10	176.0	7.20
22	Dec. 20	179.0	7.20
23	Dec. 31	182.0	7.20
24	Jan. 10	185.0	4.92
25	Jan. 20	188.0	4.92
26	Jan. 31	191.0	4.92
27	Feb. 10	194.0	6.34
28	Feb. 20	197.0	6.34
29	Feb. 28	200.0	6.34
30	Mar. 10	203.0	10.78
31	Mar. 20	206.0	10.78
32	Mar. 31	209.0	10.78
33	Apr. 10	212.0	16.57
34	Apr. 20	215.0	16.57
35	Apr. 30	218.0	16.57
36	May 10	220.0	21.4

Material Properties

The material properties used in the modeling effort were based on the information provided by the Hunan Hydroelectric Investigation and Design Institute (Zhang 1995), which consisted of foundation rock, conventional concrete, and RCC. These properties are summarized in Table 2.

The concrete modulus formula used is as follows:

$$E(\tau) = E_0(1 - e^{-m_1\tau})$$

J. Constr. Eng. Manage., 2000, 126(5): 381-388

TABLE 2. Material Properties Anticipated for RCC Dam Construction

Material property (1)	Foundation rock (2)	Conventional concrete (3)	RCC concrete 150 (4)	RCC concrete 100 (5)
Elastic modulus E_0 (kg/m^2)	2.2E9	2.6E9	4.03E9	3.0E9
Poisson's ratio μ	0.17	0.17	0.17	0.17
Surface exothermic coefficient β (J/m^2 day °C)	N/A	2.01E6	1.67E6	1.67E6
Specific heat c (kcal/kg °C)	963	942	938	837
Temperature conductivity coefficient (m^2/day)	0.1	0.096	0.096	0.096
Final adiabatic temperature increase θ_0 (°C)	N/A	28.7	17.0	14.0
Linear expansion factor (1/°C)	7.0E-6	7.0E-6	5.8E-6	6.0E-6
Gravity γ (kg/m^3)	2,700	2,400	2,480	2,480
Constant for modulus increase m_1	N/A	0.087	0.074	0.06
Constant for temperature increase m_2	N/A	0.3	0.3	0.3

Note: N/A = not available.

which is a function of concrete age τ.

The formula of temperature increase due to hydration is as follows:

$$\theta(\tau) = \theta_0(1 - e^{-m_2\tau})$$

The creep compliance relationship used is as follows:

$$C(t, \tau) = \left(A_0 + \frac{A_1}{\tau} + \frac{A_2}{\tau^2}\right)[1 - e^{-K_1(t-\tau)}] + \left(B_0 + \frac{B_1}{\tau} + \frac{B_2}{\tau^2}\right) \cdot [1 - e^{-K_2(t-\tau)}] + D[e^{-K_3\tau} - e^{-K_3 t}]$$

Creep experimental data are expensive and difficult to obtain as the duration of the experiments require long periods of time. These experiments can be accelerated for some materials. For this numerical exercise, the material constants for concrete were obtained from published data. The constants in the above function for RCC material used in the modeling analysis were obtained from experimental results of the Yantan project (Zhang 1995) as follows:

$$A_0 = 0.058864; \quad A_1 = 7.4729; \quad A_2 = -5.2079$$

$$B_0 = 0.38362; \quad B_1 = -11.115; \quad B_2 = 7.9619$$

$$K_1 = 1.356; \quad K_2 = 0.08919; \quad K_3 = 0.078675$$

$$D = 4.2808$$

The constants for the conventional concrete were obtained from the experimental results of the Dongfeng project (Zhang 1995):

$$A_0 = 0.35494; \quad A_1 = 3.7335; \quad A_2 = -2.5644$$

$$B_0 = 0.48368; \quad B_1 = -0.186; \quad B_2 = 0.13786$$

$$K_1 = 0.35361; \quad K_2 = 0.012486; \quad K_3 = 0.032642$$

$$D = 0.83509$$

Numerical Simulation of Construction

The finite-element mesh is composed of eight-node isoparametric hexahedron elements to model the section of interest of the RCC dam and rock foundation in 3D space. The schematic shown in Fig. 6 indicates the 100-m depth used to model the foundation rock and the 40-m and 80-m surface areas on the upstream and downstream sides of the dam. The RCC dam is designed to have a maximum height of 106 m at the overflow sections. The 3-m vertical thickness of the elements was determined based on the anticipated RCC lifts at average condition for a 10-day construction period. A total of 2,598 elements and 3,472 nodes were used to model the section of interest in the RCC dam including the foundation.

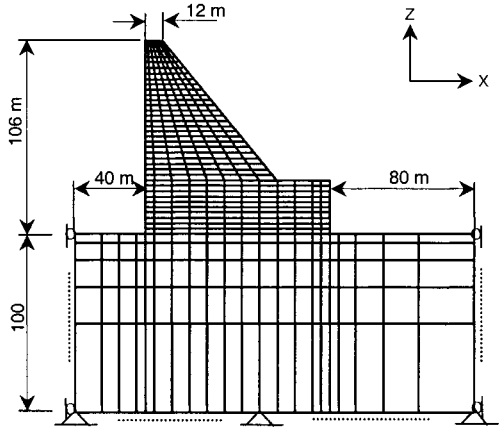

FIG. 6. Finite-Element Mesh in *X-Z*-Plane

Boundary and Initial Conditions

1. Restriction Condition for Foundation Boundaries. The foundation rock is infinite, and no horizontal movement is allowed; thus the foundation rock of this FEM is restricted in all horizontal directions (i.e., there are rollers on the vertical boundaries and pins at the bottom boundary). Therefore, the vertical direction movement is restricted in the bottom boundary.
2. Temperature Condition at Boundaries. There is a hot water layer inside the foundation rock as shown in Fig. 4 and it is 45°C. All boundaries around the foundation rock satisfy the adiabatic condition: $\partial T/\partial n = 0$ (i.e., no change in temperature in the direction normal to the plane). The dam and the foundation that are exposed to the atmosphere satisfy the following condition (as defined previously):

$$\lambda \frac{\partial T}{\partial n} = -\beta(T - T_a)$$

3. Initial Conditions. The initial temperature of all the foundation elements is calculated by interpolating between the known points at the boundaries in Item 2. The initial temperature of each layer of the dam is set to be equal to the climatic temperature at the time when it is constructed.

ANALYSIS OF RESULTS

From the temperature and stress fields produced during the construction of an RCC dam, their general patterns at a macrolevel can be summarized, and they can provide engineers basic design information.

J. Constr. Eng. Manage., 2000, 126(5): 381-388

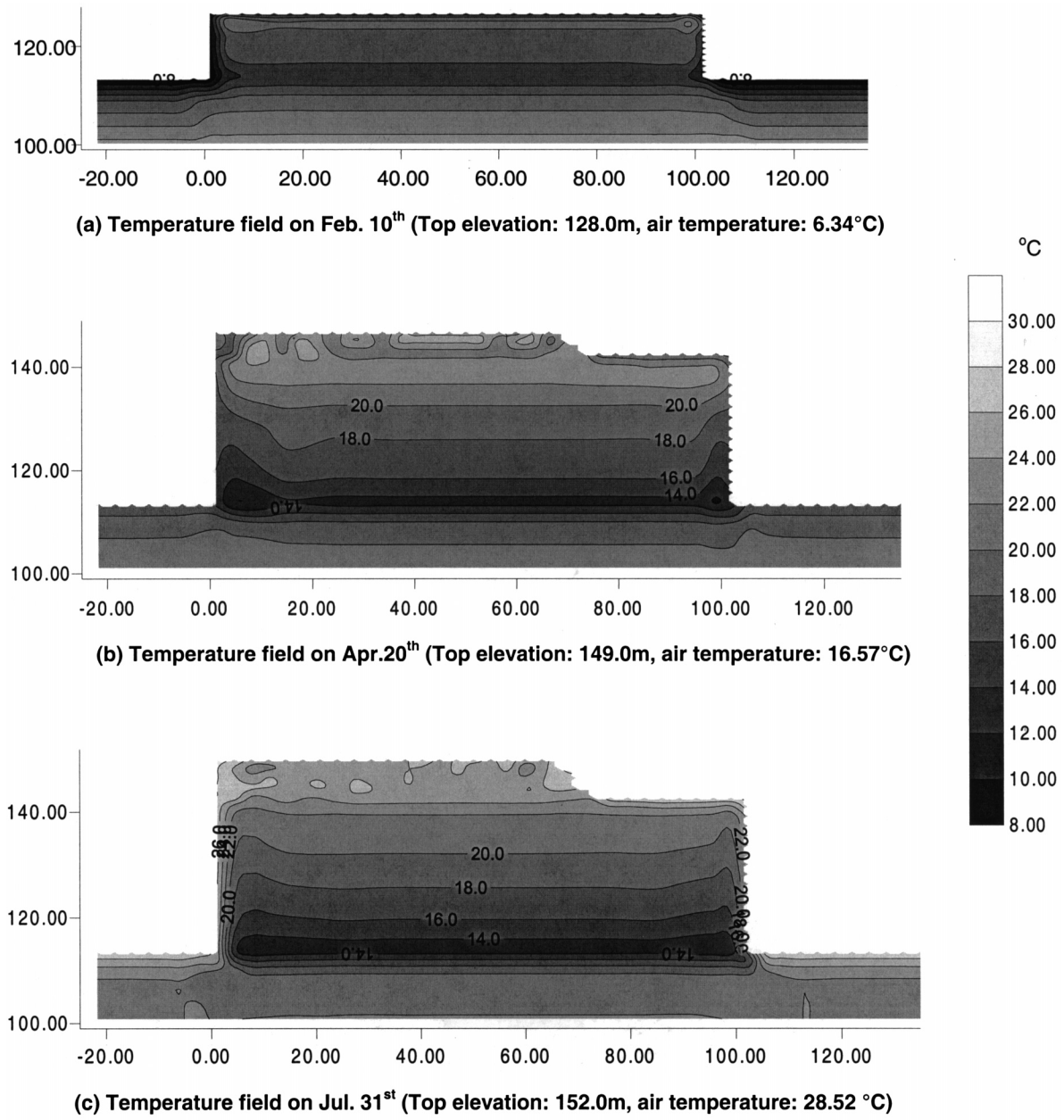

FIG. 7. Computer Simulated Temperature Field during Construction

Because the RCC dam is constructed in layers and the time interval between two layers is relatively short, heat dissipation through the dam surface has a small effect on the maximum temperature increase inside the dam body. During the cool construction months (December through April) the maximum temperature of the concrete is mainly based on the initial temperature and the adiabatic hydration temperature rise of the concrete. For example, the initial temperature of concrete built in February is 6.34°C, and the maximum temperature inside the concrete is about 18.0°C [Fig. 7(a)]. Although the initial temperature of concrete built in April is 16.57°C, the maximum temperature inside is about 28°C [Fig. 7(b)]. Therefore, it will decrease the maximum temperature of the dam if it is constructed in the low temperature seasons. This will, in turn, reduce the thermal stresses of the dam after it cools down.

As mentioned before, the construction will be stopped from May to September at an elevation of 152 m. Fig. 7(c) shows how the temperature of the dam changes due to the heat produced by hydration and the variation of the climatic temperature. Figs. 7(a–c) show that the temperature variation of the dam mainly occurs on those surfaces exposed to the atmosphere (upstream, downstream, and top surface). Specific methods such as curing and covering the surfaces with wet blankets may be needed in these areas to avoid thermal cracks.

For the stress distribution analysis, the vertical stresses are more likely to govern design compared with the horizontal and shear stresses, because during the operation the high water reservoir will produce large vertical tension stress at the upstream surface of the dam. Therefore, the vertical stress σ_z is discussed. The tension thermal stress on the top surface is relatively small ($\sigma_z < 5.0$ kg/cm^2) [Fig. 8(a)]. Thus the surface cracks will not occur if the rate of construction process is maintained and is covered with the next lift. Thermal stresses play an important role in the stress field, and the gravity load increases due to the new added lift. However, Figs. 8(b and c) show that the compression stress at the intersection of the dam/foundation at the upstream side (denoted as Point ''O'' in the figures) becomes smaller (maximum σ_z on October 10 is about -32 kg/cm^2, whereas on October 20 it is about -30 kg/cm^2). This is because the tension stress created by the tem-

J. Constr. Eng. Manage., 2000, 126(5): 381-388

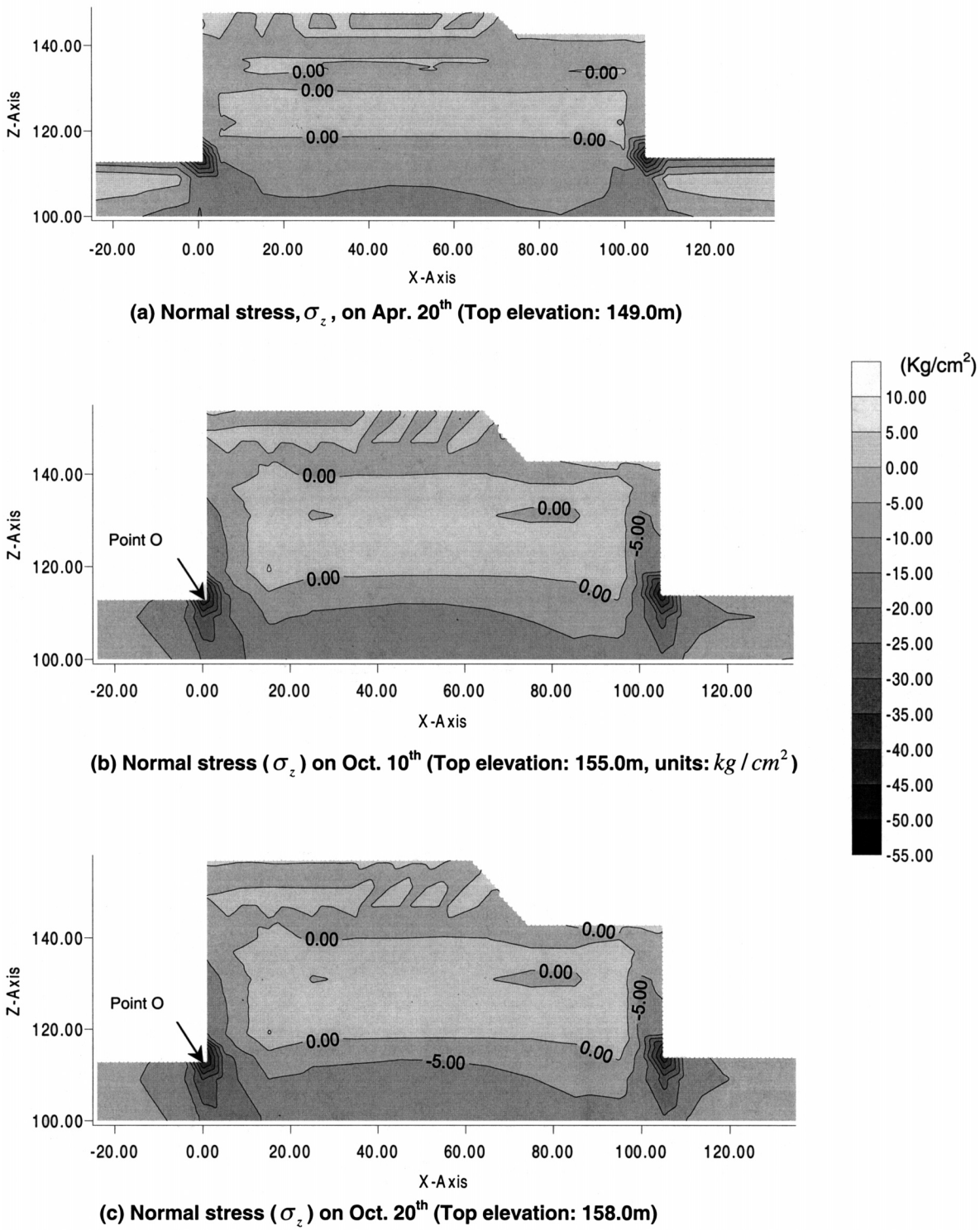

FIG. 8. Computer Simulated Normal Stress during RCC Dam Construction Sequence

perature drop is larger than the compression stress produced by the gravity. As the construction progresses, the gravity load overcomes the induced thermal tension stress.

At the end of the construction, the stress at the upstream surface of the dam is in compression (Fig. 9). It is advantageous to offset the tension stress produced by the water impoundment once the reservoir is filled and the temperature drops at the upstream face during operation. Due to the small temperature gradients between construction lifts, the induced thermal shear stresses were relatively small during the whole construction period.

CONCLUSIONS

This paper simulates the temperature and stress fields during construction of an RCC gravity dam. Based on the temperature and stress fields, some meaningful closing remarks are presented. The stress field results show that there are small tension and shear stresses, which guarantees the integrity and safety of the dam. Therefore, based on the simulation it is feasible and advantageous to build RCC dams in the low temperature seasons. First, RCC dams use less cement than conventional dams, and the adiabatic hydration temperature rise is also

J. Constr. Eng. Manage., 2000, 126(5): 381-388

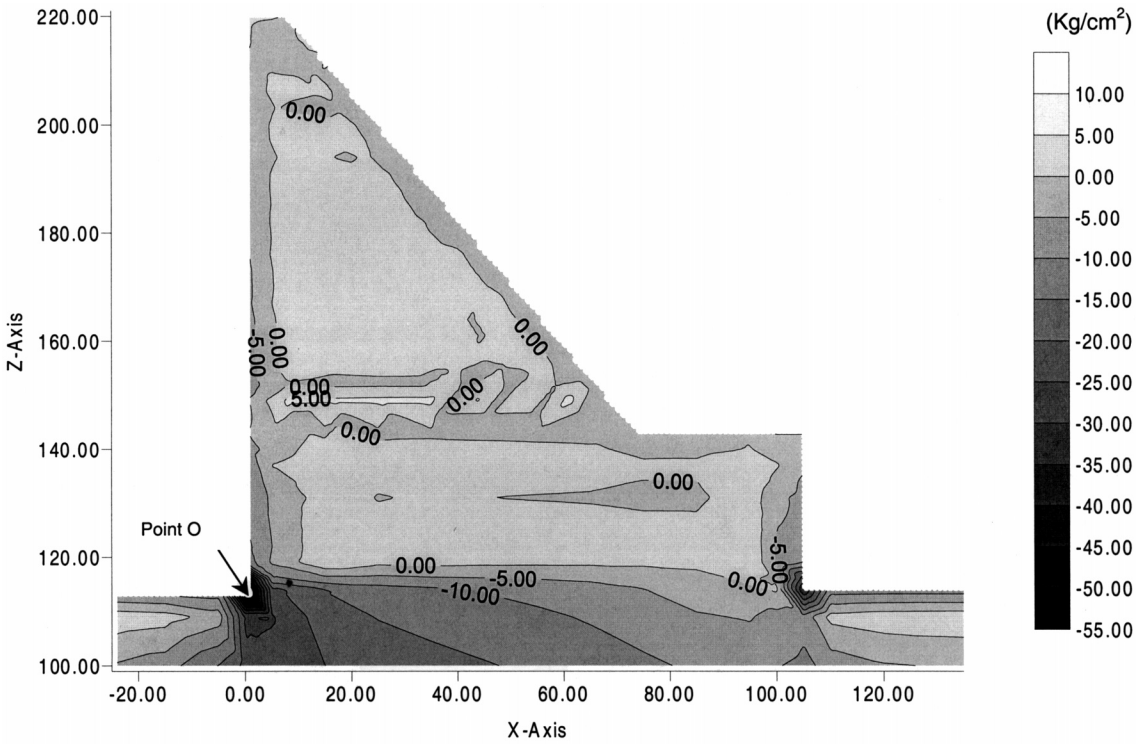

FIG. 9. Computer Simulated Normal Stress (σ_z) on May 31, Final Elevation (Top Elevation: 220 m)

smaller. This helps reduce the peak temperature inside the dam after hydration, and it also helps reduce the thermal stresses and prevents the thermal cracks. Second, no cooling methods are necessary to control the temperature, reducing the cost of the project. However, some cooling methods may be needed for the surface lifts exposed to the summer high temperature. Finally, to simulate the temperature and stress fields completely, both of these fields of the dam in operation time after the reservoir is filled with water also need to be simulated. The temperature and stress fields at the end of the construction generated by this paper provide initial conditions to analyze these fields during the operation of the dam.

Acknowledgments

The writers would like to acknowledge the contributions to this paper from their colleagues in China, Prof. Guangting Liu and Dr. Guoxin Zhang. The writers would also like to recognize the Department of Civil and Environmental Engineering at Tulane University for the financial support provided to Mr. Yong Wu during his graduate studies at that institution.

APPENDIX. REFERENCES

American Concrete Institute (ACI). (1978). ''Prediction of creep, shrinkage and temperature effects in concrete structures.'' *ACI #209-78*, 2nd Draft, Detroit.

Bazant, Z. P. (1982). ''Mathematical models for creep and shrinkage of concrete.'' *Creep and shrinkage in concrete structure*, Z. P. Bazant and F. H. Wittman, eds., Wiley, New York.

Bazant, Z. P., and Wu, S. T. (1973). ''Dirichlet series creep function for aging concrete.'' *J. Engrg. Mech. Div.*, ASCE 99(2), 367–387.

Comité Euro-International du Béton-Fédération Internationale de la Précontrainte (CEB-FIP). (1978). *Model code for concrete structures*, Paris.

Du, C. J., and Liu, G. T. (1994). ''Numerical procedure for thermal creep stress in mass concrete structures.'' *Communications in Numer. Methods in Engrg.*, 10, 545–554.

Dunstan, M. R. H. (1999). ''Recent developments in RCC dams. *Int. J. Hydropower and Dams*, U.K., 6(1), 40–45.

Hansen, K. D. (1996). ''Roller compacted concrete: A civil engineering innovation.'' *Concrete Int.*, 18(3), 49–53.

Hansen, K. D. (1997). ''Current RCC dam activity in the USA.'' *Int. J. Hydropower and Dams*, U.K., 4(5), 62–65.

Mills, A. F. (1999). *Heat transfer*, 2nd Ed., Prentice-Hall, Upper Saddler River, N.J.

Schrader, E. K. (1988). ''Roller compacted concrete.'' Chapter 18, *Advanced dam engineering for design, construction, and rehabilitation*, R. B. Jansen, ed., Van Nostrand Reinhold, New York, 540–577.

Smoack, W. G. (1991). ''Cracks repairs to Upper Stillwater Dam.'' *Concrete Int.*, 13(2), 33–36.

U.S. Army Corps of Engineers (U.S. ACE). (1992). *Roller-compacted concrete, Engr. Manual No. 1110-2-2006*, Department of the Army, Washington, D.C.

U.S. Army Corps of Engineers (U.S. ACE). (1993). ''Structural design using the roller-compacted concrete (RCC) construction process.'' *Tech. Letter No. 1110-2-343*, Department of the Army, Washington, D.C.

Wu, Y., and Luna, R. (2000). ''Temperature and creep effect on mass concrete behavior—A numerical implementation.'' *J. Appl. Finite Elements and Comp. Aided Engrg.*, in press.

Zhang, M. L. (1995). ''Study on structural treatment, stress and stability of roller compacted concrete gravity dam.'' MS thesis, Dept. of Hydr. and Hydropower Engrg., Tsinghua University, Beijing (in Chinese).

Zhu, B. F. (1985). ''The elastic modulus, creep compliance and stress relaxation coefficient of concrete.'' *Hydr. J.*, Beijing, 9(8), 56–61 (in Chinese).

Zhu, B. F., Wang, T. S., and Ding, B. Y. (1976). *Thermal stress and temperature control of hydraulic concrete structure*, Hydraulic and Electric Power Publishing House, Beijing (in Chinese).